Planar terahertz metamaterial with three-resonant frequencies*

Chen Zhi(陈 智)[a] and Zhang Ya-Xin(张雅鑫)[b]†

[a] National Key Laboratory of Science and Technology on Communication, University of Electronic Science and Technology of China, Chengdu 611731, China
[b] Terahertz Science and Technology Research Center, University of Electronic Science and Technology of China, Chengdu 610054, China

(Received 10 December 2012; revised manuscript received 4 March 2013)

In this paper, we study a three-resonant metamaterial with the combination of dual-resonant and single-resonant metamaterials. We present a new method to design multi-resonant metamaterial, which has a smaller dimension than general symmetric and asymmetric multi-resonant metamaterials. Theoretical and experimental results show that the structure has three distinct absorption frequencies centering around 0.29 THz, 0.46 THz, and 0.92 THz, and that each of them corresponds to a different resonant mode. Due to the good separation of the different resonances, this design provides a unique and effective method to construct multiband terahertz devices.

Keywords: THz-metamaterial, THz-resonator

PACS: 78.67.Pt, 42.60.Da **DOI:** 10.1088/1674-1056/22/6/067802

1. Introduction

New artificial electromagnetic material (metamaterial) is made of periodically arranged subwavelength units.[1–4] This artificial electromagnetic media can control the characteristics of transmission through designing the resonant unit.[5–10] Many materials do not inherently respond to the terahertz frequency region, however, metamaterials have special features in this region. The dimensions of the electromagnetic structure for terahertz metamaterials are of the order of micrometers, so metamaterials can be fabricated on silicon substrates using photo-etching technology, and can achieve good performance in controlling THz radiation.[11,12] Due to their customizable electromagnetic properties, metamaterials provide a promising solution for constructing terahertz functional devices, including terahertz resonators, filters, modulators, sensors, and so on.[13–18]

Recently, it has been reported that terahertz metamaterials exhibit single-band and dual-band responses.[19–24] General symmetric and asymmetric triple-resonant metamaterials as the extension of dual-band and single-band structures are also presented.[25,26] However, these structures are laterally designed structures that have difficulty in constructing multi-resonance (more than five resonances). The reason for this is that the lateral size becomes large as the number of resonances increases, which will affect the resonant intensity.

In this paper we present a particular structure of triple-resonant metamaterial, which is the lengthways combination of single-band and dual-band metamaterials. With the combination of these two structures, we can realize multi-resonant metamaterial with three absorption frequency bands. Compared with the general triple-resonant metamaterial,[23,24] this proposed structure is more compact and brings unique advantages.

2. Model and simulation of three-resonant metamaterial

The geometry of the structure is a combination of two kinds of electric inductor–capacitor (ELC) resonators, as shown in Fig. 1(a). The above part of the structure is a single-resonant metamaterial and the lower part is a dual-resonant metamaterial. The period of the structure is $L_x = L_y = 84$ μm, and the other dimensions are $A_x = A_y = 72$ μm, $g_1 = 8$ μm, $g_2 = 4$ μm, $g_3 = 4$ μm, $w_1 = 26$ μm, $w_2 = 12$ μm. The line width of the structure is $w = 4$ μm. A 500 nm aluminum film is deposited on one side of silicon and then patterned into the designed shape by photo-etching, as shown in Fig. 1(b). The photographs of four unit cells and a portion of the fabricated three-resonant metamaterials are shown in Figs. 2(a) and 2(b), respectively. The light area on the figure is the aluminum film and the dark area the 500 μm silicon substrate that we can observe directly.

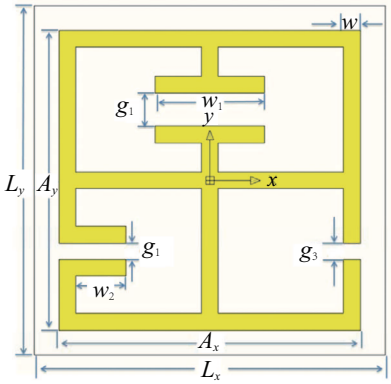
The unit cell was simulated utilizing a commercial finite difference time domain (FDTD) solver, CST's Microwave Studio, in which the metamaterial was designed and analyzed. The polarization of the incident wave's electric field is perpendicular to the split gaps. The results show that the surface current simulated by the line polarization incident wave in the structure has different characteristic distributions corresponding to different resonant frequencies, as demonstrated in Fig. 3. It can be found that there are three different resonant circuits. At 0.29 THz, the surface current mainly concentrates on the middle pole of the under dual-resonant structure to form

*Project supported by High-Tech Research and Development (863) Program of China (Grand No. 2011AA010201) and the National Natural Science Foundation of China (Contract No. 61001031).

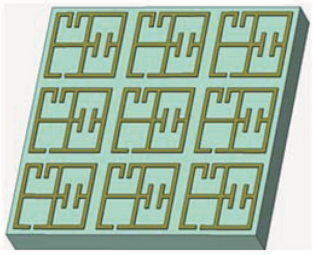
†Corresponding author. E-mail: zhangyaxin@uestc.edu.cn

© 2013 Chinese Physical Society and IOP Publishing Ltd

a circuit. At the second resonant frequency of 0.46 THz, the surface current flows through the upper single-resonant structure and the lower-left resonant loop of the lower part of the structure. When the surface current flows through the whole unit, as shown in Fig. 3(c), the resonance is at the highest frequency position of 0.92 THz.



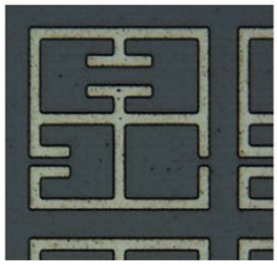
(a)



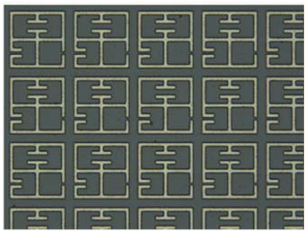
(b)

Fig. 1. (color online) The three-resonant metamaterial: (a) the designed three-resonant unit cell with geometries, and (b) the designed three-resonant period arrays on the silicon substrate.

In Fig. 4, the results show the relation between the distribution of the electric field and the resonant frequency. It can be found that around the frequency 0.29 THz, the electric field intensities are very strong in the two split gaps of the under dual-resonant structure. At the 0.46 THz frequency, the electric field concentrates in the lower-left split gap and the upper split gap. At the highest frequency of 0.92 THz, there are strong electric field distributions in the three split gaps. The surface current and electric fields clearly demonstrate that, in contrast to general multi-resonant metamaterial, in this structure the resonant frequencies are not the only response to the single split gap. The mutual coupling between the different gaps and circuits plays a very important role in this structure.



(a)

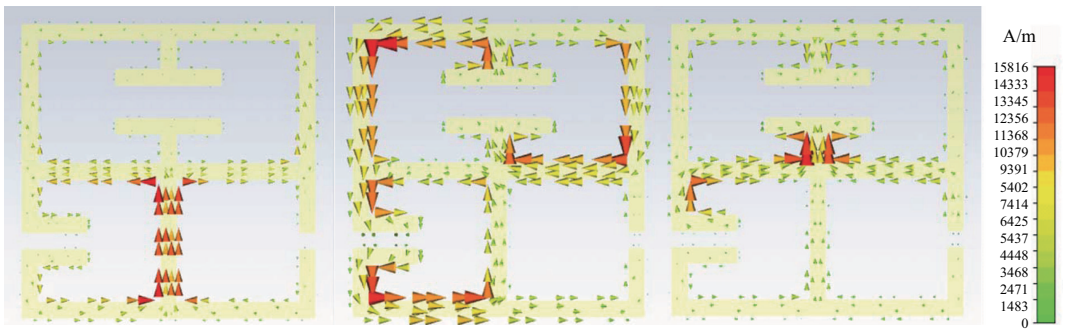


(b)

Fig. 2. (color online) The three-resonant fabricated sample: (a) a unit cell of the fabricated sample, and (b) a photomicrograph of a portion of the fabricated three-resonant metamaterial.

3. Experimental results

Terahertz time-domain spectroscopy (THz-TDS) was used to characterize the performance of the metamaterial device. For this THz-TDS experimental system, a Ti:Sa femtosecond laser source delivering 80-fs pulses at a 790-nm central wavelength is applied for the generation and detection of terahertz radiation. The excitation of the emitter (a GaAs photoconductive antenna) with ultrashort laser pulses results in a burst of subpicosecond pulses with frequencies spanning from 0.1 THz to 3.0 THz. A polyethylene lens focuses



(a) (b) (c)

Fig. 3. (color online) The circular surface current distribution of the designed three-resonant metamaterial. (a) Near the lowest resonant frequency of 0.3 THz, (b) near the middle resonant frequency of 0.5 THz, and (c) near the highest resonant frequency of 0.92 THz.

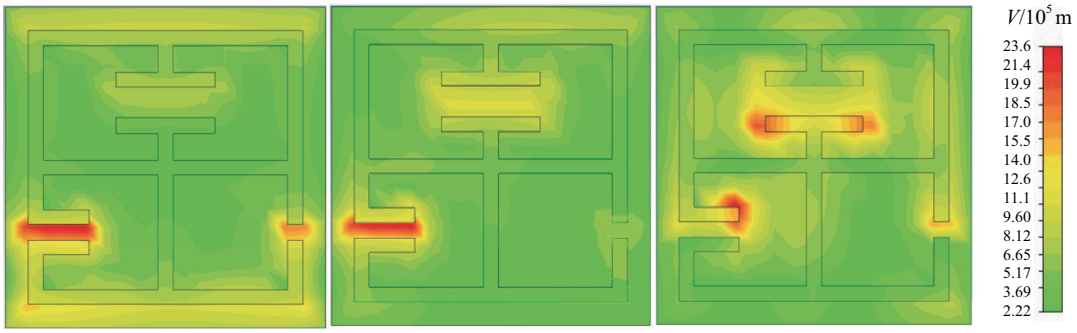


Fig. 4. (color online) The electric field distribution of the designed three-resonant metamaterial near different resonant frequencies. (a) Near the resonant frequency of 0.3 THz, (b) near the resonant frequency of 0.5 THz, and (c) near the resonant frequency of 0.92 THz.

the linearly polarized THz beam onto the metamaterial sample at a diameter of about 2 mm, and a second polyethylene lens recollimates the transmitted THz beam, which is directed to a photoelectric crystal. The experiments were performed at a room temperature of 23 °C in a dry air atmosphere, and the metamaterial sample was placed in the transmission THz-TDS with a linear polarization incident terahertz wave. All the experiments were performed at perpendicular incidence with the terahertz electric and magnetic field lying in-plane. The time-varying electric field of the THz signal was recorded, and the electric field spectral amplitude and phase were directly obtained by fast Fourier transformation (FFT) analysis.

The simulation results of the transmission rate can be obtained by CST's Microwave Studio. A linear polarized plane wave was set to incident on the structure, and a time domain solver was used. A bare silicon substrate was chosen to be the reference of the measurement and the complex transmission as a function of frequency by dividing the Fourier transformed sample and reference waveforms. The polarization of the electric field was perpendicular to the split gaps to stimulate three different modes at 0.295 THz, 0.475 THz, and 0.92 THz. Figure 5 shows the experimental and simulation results. Figures 5(a) and 5(b) are the original experimental results, and figure 5(c) is the comparison between the simulation and experimental results. Figure 5(a) shows the original experimental time-domain waveform of air, silicon, and the three-resonant metamaterial with the THz-TDS system mentioned above. Figure 5(b) is the experimental frequency spectrum of air, silicon, and metamaterial, which is the FFT of the original experimental time-domain waveforms. Based on the experimental data shown in Figs. 5(a) and 5(b) with respect to a suitable reference, which in this case is a bare silicon substrate, allows the determination of the complex transmission as a function of frequency by dividing the Fourier transformed sample and reference waveforms, and we can get the transmission rate as shown in Fig. 5(c). The experimental transmission rate in Fig. 5(c) (the solid red line) shows that there are three distinct transmission minima at 0.295 THz, 0.475 THz, and 0.92 THz. Compared to the simulation results, they agree well with each other, and the errors of the measurement for the transmission frequencies are 1.7%, 3.2%, and 2.2%. These results show that the experimental results agree with the simulation results.

However, there are some differences between the experimental results and simulations. The transmission rate of the experimental result is higher than that of the simulation at 0.475 THz and 0.92 THz. Also, the bandwidth of the resonance peak in the experimental results is larger than the simulation. The following four reasons cause these differences. First, the resonant frequency and bandwidth are extremely sensitive to the size of this structure, and the mismachining tolerance causes the differences in the width of the gaps, which will lead to the frequency shift and bandwidth change. Second, in the simulation, considering the number of meshes and the computing duration, only a 3×3 array has been modeled and simulated. Moreover, the ideal plane wave and open space boundary have been applied. In the experiment, however, there are thousands of units in the manufactured sample and the boundary of the sample is not an ideal smooth transition to the free space. The mutual effect among such a large number of units is much stronger than that in the simulation, and boundary discontinuity will cause the bandwidth change and resonant frequency shift. Third, in the simulation, the polarization of the incident plane wave is absolutely perpendicular to the gaps of the unit. In the experiment, however, the incident wave is the quasi-plane wave and the polarization of the electric field cannot be set strictly perpendicular to the split gaps, which will affect the bandwidth of the resonance frequency in the experimental results. Finally, the difference is also due to the silicon substrate and the depth of the coated 300 nm-thick metal surface. Ideal material factors have been used in the simulation, while the material factors and the characteristics of the silicon substrates are different in the experiment. Furthermore, there is minor mismatching tolerance in the process of coating the film.

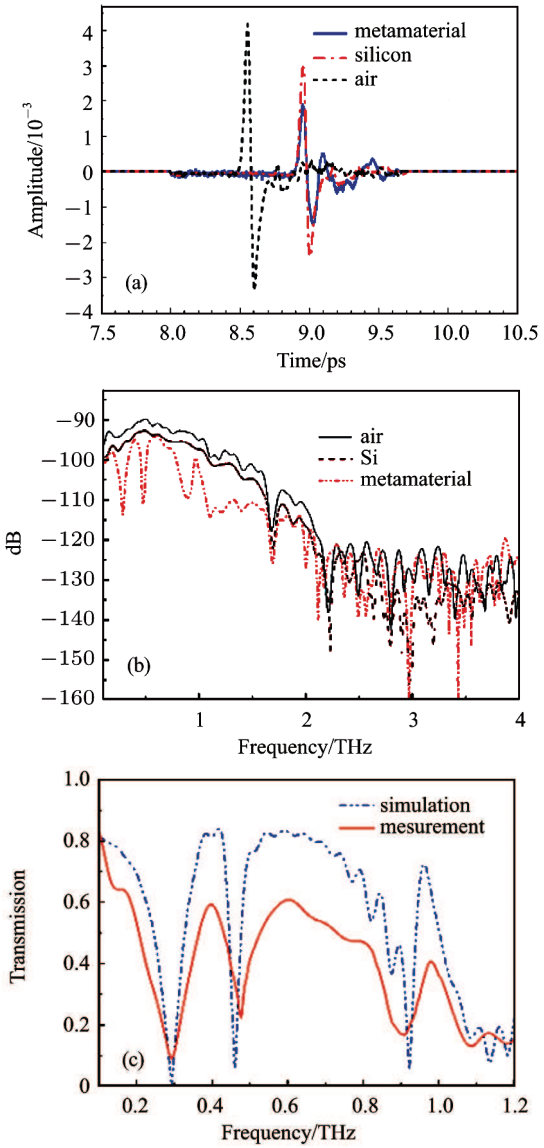


Fig. 5. (color online) The results of the simulation and experiment: (a) the time-domain waveforms of air, silicon, and the three-resonant metamaterial measured by THz-TDS, (b) the frequency spectrum of air, silicon, and the metamaterial, and (c) the simulated and measured transmissions of the metamaterial sample.

4. Conclusions

In conclusion, we presented the design, simulation, and measurement of a three-resonant metamaterial with composite structure that is different from conventional multi-resonant metamaterial structures. Theoretical and experimental results show that the structure has three distinct absorption positions near 0.29 THz, 0.46 THz, and 0.92 THz. Compared with the three-resonant metamaterial in Refs. [25] and [26], which are a parallel arrangement of dual-band and single-band structures, the proposed structure is a dislocation arrangement of such structures and will realize multi-resonant metamaterial (more than five resonances) with a more compact structure. Moreover, the resonances in the former are caused by a separate LC resonance of each independent split-gap circuit; in the proposed structure, mutual coupling between different split-gaps and circuits plays a very important role in the resonance, which will realize multi-band resonance with better performance. This terahertz three-resonant metamaterial may have potential use in building multi-band filters, modulators, switches, and so on.

References

[1] Smith D R, Padilla W J, Vier D C, Nemat-Nasser S C and Schultz S 2000 *Phys. Rev. Lett.* **84** 4184
[2] Pendry J B, Schuring D and Smith D R 2006 *Science* **312** 1780
[3] Walser R M 2001 *Proc. SPIE* **4467** 1
[4] Cummer S A and Popa B I 2004 *Appl. Phys. Lett.* **85** 4564
[5] Tsai Y J, Larouche S, Tyler T, Lipworth G, Jokerst N M and Smith D R 2011 *Opt. Express* **19** 24
[6] O'Hara J F, Smirnova E, Azad A K, Chen H T and Taylor A J 2007 *Active and Passive Electronics* **10** 1155
[7] Lim C S, Hong M H, Chen Z C, Han N R, Luk'yanchuk B and Chong T C 2010 *Opt. Express* **18** 12
[8] Chen Z C, Hong M H, Lim C S, Han N R, Shi L P and Chong T C 2010 *Appl. Phys. Lett.* **96** 181101
[9] Tao H, Strikwerda A C, Fan K, Padilla W J, Zhang X and Averitt R D 2009 *Phys. Rev. Lett.* **103** 147401
[10] Chen W C, Totachawattana A, Fan K, Ponsetto J L, Strikwerda A C, Zhang X, Averitt R D and Padilla W J 2012 *Phys. Rev. B* **85** 035112
[11] Tao H, Landy N L, Bingham C M, Zhang X, Averitt R D and Padilla W J 2008 *Opt. Express* **16** 007181
[12] Azad A K, Taylor A J and Smirnova E and O'Hara J F 2008 *Appl. Phys. Lett.* **92** 011119
[13] Chen H T, Padilla W J, Zide J M O, Gossard A C, Taylor A J and Averitt R D 2006 *Nature* **444** 597
[14] Chen H T, Padilla W J, Zide J M O, Rank S R, Gossard A C, Taylor A J and Averitt R D 2007 *Opt. Lett.* **32** 001620
[15] Chen H T, Padilla W J, Cich M J, Azad A K, Averitt R D and Taylor A J 2009 *Nat. Photon.* **3** 148
[16] Shen N H, Kafesaki M, Koschny T, Zhang L, Economou E N and Soukoulis C M 2009 *Phys. Rev. B* **79** 161102
[17] Shrekenhamer D, Rout S, Strikwerda A C, Bingham C, Averitt R D, Sonkusale S and Padilla W J 2011 *Opt. Express* **19** 10
[18] Withayachumnankul W and Abbott D 2009 *IEEE Photon. J.* **1** 99
[19] Yuan Y, Bingham C, Tyler T, Palit S, Hand T H, Padilla W J, Smith D R, Jokerst N M and Cummer S A 2008 *Opt. Express* **16** 9746
[20] Yuan Y, Bingham C, Tyler T, Palit S, Hand T H, Padilla W J, Smith D R, Jokerst N M and Cummer S A 2008 *Appl. Phys. Lett.* **93** 191110
[21] Wang J F, Qu S B, Yang Y M, Ma H, Wu X and Xu Z 2009 *Appl. Phys. Lett.* **95** 014105
[22] Lin M Q and Cui T J 2008 *IEEE Microw. Wirel. Co.* **18** 245
[23] Xiong H, Hong J S and Jin D L 2012 *Chin. Phys. B* **21** 124101
[24] Fan J, Sun G Y and Zhu W R 2011 *Chin. Phys. B* **20** 114101
[25] Zhang Y X, Qiao S, Huang W X, Ling W and Li L 2011 *Appl. Phys. Lett.* **99** 073111
[26] Zhang Y X, Qiao S, Zhao T, Ling W and Liu S 2012 *Prog. Electromag. Res.* **125** 21